Melting and freezing behavior of indium metal in porous glasses

K. M. Unruh
Department of Physics and Astronomy, University of Delaware, Newark, Delaware 19716

T. E. Huber
Laser Research, Howard University, Washington, D.C. 20059
and Department of Physics, Polytechnic University, Brooklyn, New York 11201

C. A. Huber
Naval Surface Warfare Center, Silver Spring, Maryland 20903-5000
(Received 19 April 1993)

The size-dependent melting and freezing behavior of In metal in porous silica glasses with mean pore diameters between 6 and 141 nm has been studied by differential scanning calorimetry. The melting and freezing temperatures of the pore In were always less than the corresponding bulk values, and varied in inverse proportion to the diameter of the confining silica pores. In the smallest pores the latent heat of fusion was also determined, and found to be about one-third of its bulk value. The observed size dependence of the melting temperature was in good agreement with the predictions of thermodynamic treatments of melting in finite systems, and allowed the solid-liquid interfacial free energy to be estimated for several different geometrical models. The measured latent heat, however, was smaller than expected based on thermodynamic considerations. No evidence for an energy barrier separating the solid from the liquid was found.

INTRODUCTION

The melting and freezing behavior of finite systems has been of considerable theoretical and experimental interest for many years.[1] As early as 1888, for example, J.J. Thomson suggested that the freezing temperature of a finite particle would depend on the physical and chemical properties of the surface.[2] It was not until 1909, however, that an explicit expression for a size-dependent solid-liquid coexistence temperature first appeared.[3] By considering a system consisting of small solid and liquid spheres of equal mass in equilibrium with their common vapor, it was shown that the temperature of the triple point was reduced in inverse proportion to the particle size. A similar conclusion was later reached based on the conditions for equilibrium between a solid spherical core and a thin surrounding liquid shell.[4]

Systematic experimental studies of the melting and freezing behavior of small particles first began to appear in the late 1940s and early 1950s: first in a series of experiments on the freezing behavior of isolated *micrometer-sized* metallic droplets,[5] and later in an electron-diffraction study of the melting and freezing temperatures of vapor-deposited discontinuous films consisting of *nanometer-sized* islands of Pb, Sn, and Bi.[6] These studies demonstrated that small molten particles could often be dramatically undercooled, and that solid particles melted significantly below their bulk melting temperature.

Since the original experiments described above, the melting and freezing behavior of small particles has been studied in a variety of sample configurations and by a number of experimental techniques. Micrometer-sized particles have been prepared in the form of fine dispersions and powders, and have been studied by optical, dilatometric, calorimetric, and spectroscopic techniques.[7–9] The nanometer-sized metallic islands characteristic of discontinuous films have been studied by transmission electron microscopy and electron diffraction,[10–20] and by light-scattering measurements.[21] Nanometer-sized Sn and Bi particles embedded in sputter-deposited amorphous silica films, and bulk Sn-Ge and Pb-Ge nanocomposites prepared by mechanical attrition, have been studied by differential scanning calorimetry.[22,23] Lead precipitates in an Al single crystal have been studied by x-ray diffraction,[24] while individual Au and Ag particles deposited on the tip of a W field emitter have recently been studied by a field-emission technique.[25]

Small "particles" can also be obtained by confining a solid or liquid within the nanometer-sized pores of porous glasses. Porous silica glasses have often been used for this purpose because of their relatively well-characterized pore structures, large specific pore volumes, and commercial availability over several orders of magnitude in the mean pore diameter.[26,27] These unique properties have been exploited in a number of previous calorimetric studies of simple *nonmetallic* systems such as hydrogen,[28–30] deuterium,[28] helium,[31–33] neon,[28] and xenon,[34] as well as more complex inorganic and organic materials such as water,[34–37] *cis*- and *trans*-decalin,[38] benzene,[35,36,38] chlorobenzene,[38] naphthalene,[35,38], *p*-nitrotoluene,[35] and several alkanes.[38,39]

In this paper we report the results of a differential scanning calorimetry study of the size-dependent melting and freezing behavior of In in porous silica glasses. This work has been motivated by our interest in studying a metallic element for comparison with previously studied

0163-1829/93/48(12)/9021(7)/$06.00

nonmetallic systems, and to our knowledge is the first such study of this kind. Earlier studies of the melting and freezing behaviors of small In particles have been restricted to discontinuous films and electron microscopy measurements.[12,13,15,16,19] The freezing behavior of larger In droplets has also been briefly described.[40]

EXPERIMENT

The porous silica glasses used in this work were obtained from Controlled-Pore Glass Inc. (CPG) in the form of 200/400 mesh glass powders,[27] and from Corning Glass Works in the form of a monolithic Vycor (Corning 7930) glass rod.[41] Pore volumes and surface areas of the CPG glasses were supplied by CPG based on the results of Hg intrusion porosimetry and nitrogen adsorption measurements. Similar information on the Vycor glass was supplied by Micromeritics Instrument Corp.[42] Mean pore diameters d were estimated from the Hg intrusion measurements through the relation

$$d = -\frac{4\gamma_{lv}}{P}\cos\theta_{lw} , \quad (1)$$

where $\gamma_{lv}=480$ mJ/m^2 is the liquid-vapor surface tension of Hg, $\theta_{lw}=130°$ is the contact angle between liquid Hg and a silica wall, and P is the pressure at which liquid Hg enters cylindrical pores of diameter d.[27] Based on Eq. (1), the mean pore diameters of the CPG glasses ranged from 8.2 ± 0.6 to 141 ± 11 nm where 80% of the pore diameters fall within the quoted uncertainty. Due to the high pressures required to force Hg into very small pores, the mean pore diameter of the Vycor glass was determined from nitrogen desorption measurements, and was found to be about 5.6 ± 0.9 nm with the uncertainty corresponding to the full width at half maximum of the pore size distribution. It should be noted that Hg intrusion measurements on porous silica glasses actually measure the neck size in a connected network of only roughly cylindrical pores, and Eq. (1) provides a lower bound estimate of the mean pore diameter.

A hydraulic diameter can also be estimated from the ratio of the total pore volume to the total surface area. The hydraulic diameter was generally larger than the corresponding Hg-intrusion-determined diameter, except in the case of the smallest pores which, as noted earlier, were difficult to completely fill with Hg. In the following discussions, Hg-intrusion-based pore diameters have been used for the CPG glasses, and the nitrogen-absorption-based pore diameter has been used for the Vycor glass. The relevant physical properties of each porous glass have been summarized in Table I.

In order to simplify the process of filling the CPG glass pores with molten In, small disks of compacted powder were initially prepared at a pressure of about 1 kbar. Previous studies have shown that these compacting pressures do not alter the pore structure of porous silica powders.[43] In the case of the porous Vycor glass, thin disks were cut from a solid monolithic rod. These disks were then loaded into an externally heated high pressure reactor, and molten In at a temperature of 575 K was forced into the pores at a pressure of 4 kbar. The resulting samples contained a substantial amount of external nonpore bulk In. The high-pressure reactor used in the preparation of these, and other pore metals, semimetals, and semiconductors has been described in greater detail elsewhere.[44] Small-angle x-ray and neutron-scattering measurements have shown that the pore structure is not significantly affected by the injection process.[45]

The crystal structure of the pore In could not be determined in the case of the In-CPG samples because x-ray-diffraction spectra were dominated by the external nonpore bulk. It was possible, however, to remove most of the bulk In in the In-Vycor samples. In these samples, x-ray-diffraction measurements indicated that the pore In retained the bulk tetragonal crystalline structure, but with a uniform lattice expansion of about 0.5%.[45] The average pore In crystallite size was also estimated from the x-ray linewidth and found to be about 20 nm, considerably greater than the pore size. Given the similarity of the CPG and Vycor glasses, we do not expect significant structural differences between the In-CPG and In-Vycor samples.

A Perkin-Elmer DSC7 (differential scanning calorimeter) was used to determine melting temperatures, freezing temperatures, and latent heats of fusion by measuring the heat absorbed or released at the solid-liquid transition.[46] The temperature scale of the DSC was calibrated at a heating rate of 10 K/min to the melting temperatures of pure bulk In and Bi. The temperature scale at heating rates other than 10 K/min was appropriately corrected. The background of each raw DSC spectrum was subtracted based on a second-order polynomial fit to the measured heat flow well away from any signal of interest. Melting and freezing temperatures were than determined by extrapolating the leading edge of the heat-flow signal to the subtracted background. The heat-flow rate was calibrated to that of pure In, and latent heats were determined based on the scaled area under the melting and freezing signals. Melting and freezing temperatures were typically reproducible to within several tenths of a degree, and latent heats were reproducible to better than 5%.

All of the samples were initially stored under dry ice or liquid nitrogen in order to slow the anticipated extrusion of In from the silica pores. After a complete set of measurements, selected samples were remeasured after being stored at room temperature for several months. No

TABLE I. Summary of the physical properties of the porous silica glasses used in this study.

Glass type	d (nm)	Pore volume (cm^3/gm)	Surface area (m^2/gm)
Vycor	5.6 ± 0.9	0.16	170.5
CPG	8.2 ± 0.7	0.37	244.5
CPG	12.8 ± 0.7	0.80	141.2
CPG	18.2 ± 0.9	0.97	112.7
CPG	24.2 ± 0.9	0.89	79.0
CPG	34 ± 2	0.97	67.5
CPG	81 ± 8	1.04	27.6
CPG	101 ± 9	0.79	21.8
CPG	141 ± 11	0.95	15.6

significant differences were observed in the melting and freezing characteristics of these samples in comparison to the earlier measurements. For a given sample, repeated DSC scans through the solid-liquid transition resulted in a slight monotonic increase in the area under the bulk In melting peak in comparison to the area under the pore In peak. These results were taken as evidence of a slow extrusion of molten In from the glass pores at elevated temperatures.

EXPERIMENTAL RESULTS

Figure 1 shows the evolution in the DSC patterns of several representative In-CPG samples and an In-Vycor sample obtained at a heating rate of 10 K/min. Several features of Fig. 1 are worth noting. In the first instance, each scan contains a strong and relatively sharp endothermic peak whose position is independent of the confining pore diameter. This signal corresponds to the melting of bulk In surrounding the porous glass. In addition to the bulk melting peak, a pore-size-dependent endothermic signal was also observed. This signal corresponds to the melting of the pore In, and shifts to lower temperatures, systematically broadens, and becomes increasingly asymmetric as the pore size is reduced. Figure 2(a) summarizes the size dependence of the pore In melting temperature for all the samples studied.

The increasing reduction in the melting temperature of the pore In results in a complete separation of the bulk and pore In melting signals for the smallest pore sizes. In two of these samples it was possible to estimate the mass of the pore In. Based on the value of the bulk latent heat, the mass of the nonpore In was determined from the area under the high-temperature melting peak. By subtracting this value from the measured total In mass, the mass of the pore In was determined. This value was then used to estimate the latent heat of the pore In. For the 8.2- and 18.2-nm-diameter In-CPG samples, this analysis resulted in a pore In latent heat of 10.2 ± 0.4 and 14.7 ± 0.2 J/gm, respectively, based on repeated measurements through the melting transition. These values are significantly less than the bulk latent heat of 28.4 J/gm.[47]

Two of the melting endotherms shown in Fig. 1. have been reproduced with their corresponding freezing exotherms in Fig. 3. The offset to lower temperatures of the bulk In freezing signal in comparison to the melting signal was observed in all of the samples studied, and is the result of a small temperature lag between the actual sample temperature and the measured calorimeter temperature. The shift in the bulk In freezing temperature of about 3 K is twice the sample-calorimeter temperature

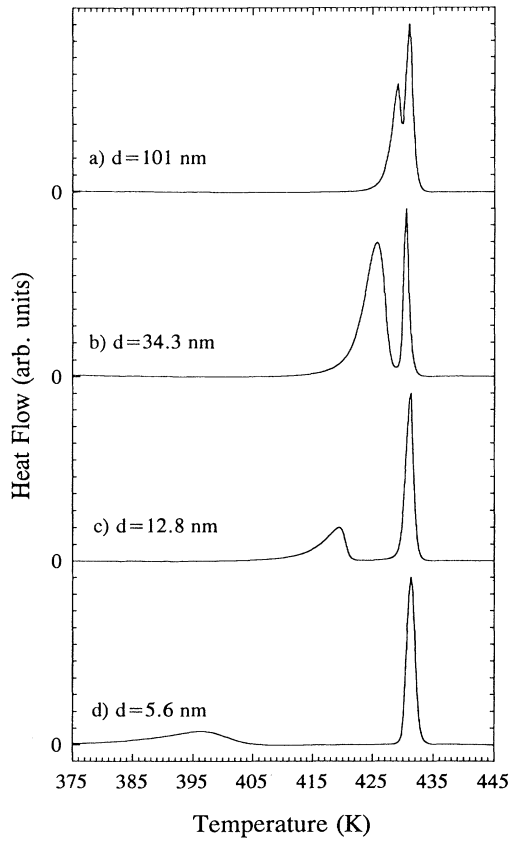

FIG. 1. Representative background-subtracted DSC melting scans for (a)–(c) In-CPG and (d) In-Vycor samples. Each scan was carried out at a heating rate of 10 K/min.

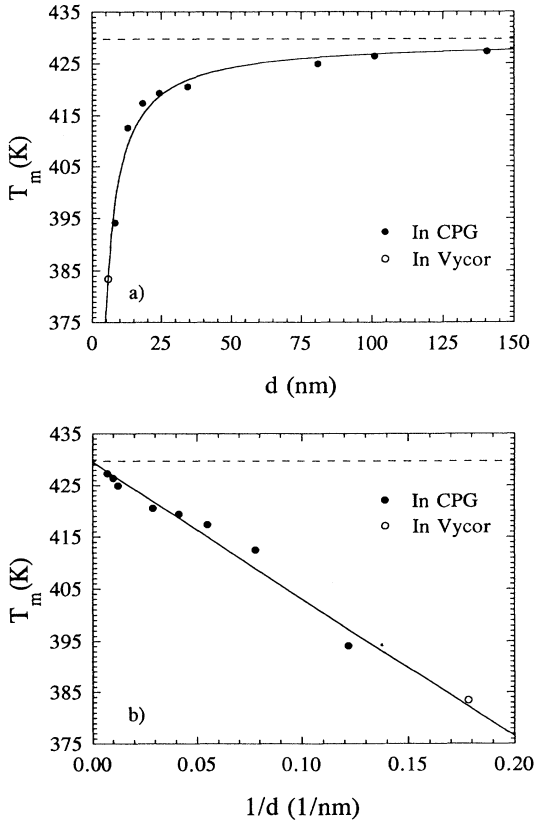

FIG. 2. (a) The melting temperature of pore In as a function of the mean pore diameter. (b) The melting temperature of pore In as a function of the inverse pore diameter. The dashed line is the melting temperature of bulk In, and the solid line through the data points is a best fit to the data as described in the text.

difference. With decreasing pore size the temperature interval between the freezing of the pore and bulk In increases slightly more rapidly than does the same interval on melting. This effect appears to be independent of the cooling rate, at least for cooling rates between 10 and 50 K/min.

DISCUSSION

No unique thermodynamic melting temperature can be defined for the solid-liquid transition in a finite system. Within the context of a thermodynamic criterion for melting and a specified geometrical model, however, certain characteristic temperatures can be associated with this process. Two closely related melting criteria, and their corresponding characteristic temperatures, will be discussed and compared with the data of Fig. 2(a). The model system will consist of a confined spherical or cylindrical "particle" of radius r at fixed volume in equilibrium with a heat reservoir at temperature T. The specific densities of the solid and liquid will be assumed equal, and both phases will be considered incompressible.

The first approach to the melting of a finite system is closely related to the classical treatment of nucleation in an undercooled melt,[8] and focuses on the change in the Helmholtz free energy δF when a portion of a solid particle is converted to liquid.[48,49] For a spherical particle with a solid core of radius r_s surrounded by a liquid shell of thickness $t \equiv r - r_s$, as shown in Fig. 4(a), one obtains

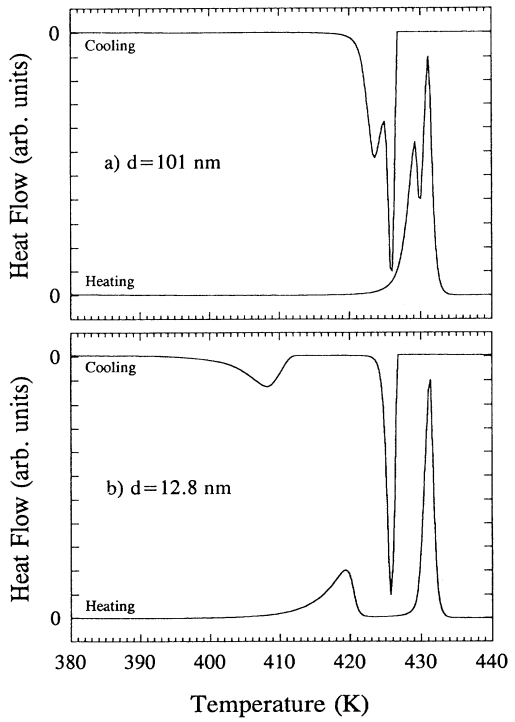

FIG. 3. Representative background-subtracted DSC melting and freezing scans for (a) $d=101$ nm, and (b) $d=12.8$ nm In-CPG samples. Each scan was carried out at a rate of 10 K/min.

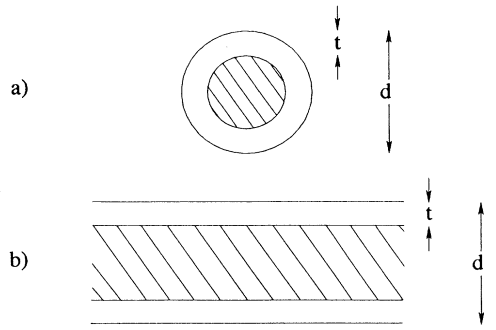

FIG. 4. The two geometries used to calculate the size dependence of the melting temperature. Solid material has been represented by the diagonal fill lines.

$$\delta F(\text{sphere}) = -\tfrac{4}{3}\pi r_s^3 L_0 \tau + 4\pi r_s^2 f_{sl} + \tfrac{4}{3}\pi r^3 L_0 \tau - 4\pi r^2 f_{sl} , \quad (2)$$

where f_{sl} is the free energy per unit area of the solid-liquid interface and the temperature dependence of the solid-liquid free-energy difference per unit volume has been approximated in terms of the bulk latent heat L_0 and bulk melting temperature T_0 as $f_l - f_s \approx L_0(T_0 - T)/T_0 \equiv L_0\tau$. Ignoring end effects, for the free-energy difference per unit length the cylindrical geometry of Fig. 4(b) yields

$$\delta F(\text{cylinder}) = -\pi r_s^2 L_0 \tau + 2\pi r_s f_{sl} + \pi r^2 L_0 \tau - 2\pi r f_{sl} . \quad (3)$$

Equations (2) and (3) have been plotted in Fig. 5 for a 10-nm-radius particle and several different values of the reduced temperature τ.

Figure 5 suggests that two different temperatures should be associated with the solid-liquid transition when a liquid layer is assumed to form surrounding a solid core. The first is that temperature at which the free energy of the completely liquid particle is just equal to the free energy of the completely solid particle, and in reduced units is given by $\tau_1(\text{sphere}) = 3f_{sl}/L_0 r$ and $\tau_1(\text{cylinder}) = 2f_{sl}/L_0 r$. The experimental observation that pore In melts below the melting temperature of bulk In indicates that $f_{sw} - f_{lw} - f_{sl} > 0$, and it is therefore energetically favorable to replace a single solid-wall interface with both liquid-wall and solid-liquid interfaces. As has been noted previously,[19,48] τ_1 represents a thermodynamic lower bound on the melting temperature.

At low temperatures, Eqs. (2) and (3) exhibit maxima of $\delta F^* \equiv \delta F(r = r^*)$ which occur at a solid core radius $r_s^*(\text{sphere}) = 2f_{sl}/L_0\tau$ and $r_s^*(\text{cylinder}) = f_{sl}/L_0\tau$. With increasing temperature the energy barriers

$$\delta F^*(\text{sphere}) = \frac{16}{3}\frac{\pi f_{sl}^3}{L_0^2 \tau^2} + \tfrac{4}{3}\pi r^3 L_0 \tau - 4\pi r^2 f_{sl} \quad (4)$$

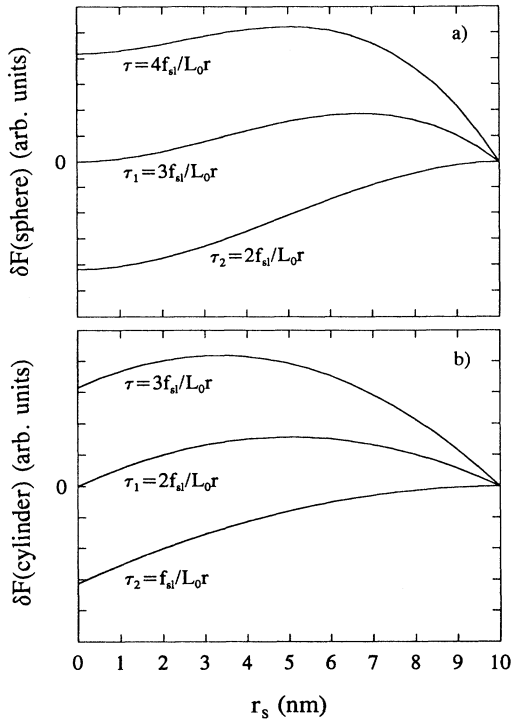

FIG. 5. The shift in the Helmholtz free energy of a particle consisting of a solid core surrounded by a liquid layer with respect to the free energy of a completely solid particle for (a) a spherical particle and (b) a cylindrical particle.

and

$$\delta F^*(\text{cylinder})=\frac{\pi f_{sl}^2}{L_0\tau}+\pi r^2 L_0\tau-2\pi r f_{sl} \tag{5}$$

separating the solid from the liquid continuously decrease and vanish at the reduced temperature $\tau_2(\text{sphere})=2f_{sl}/L_0r$ and $\tau_2(\text{cylinder})=f_{sl}/L_0r$. τ_2 represents a thermodynamic upper bound on the melting temperature.[19,48]

Between τ_1 and τ_2 the transition from the solid to the liquid is governed by kinetic as well as thermodynamic factors. In particular, the actual transition will be weighted toward τ_2 for smaller particles, and τ_1 for larger particles. Both characteristic temperatures are inversely proportional to the particle size, and reduce to the bulk melting temperature as $r\rightarrow\infty$.

A related approach to the melting of finite systems focuses on the chemical potentials $\mu_s(T,P_s)$ and $\mu_l(T,P_l)$ of the solid and liquid phases, and defines the melting temperature as that temperature at which the chemical potential of the solid core is equal to that of the surrounding liquid.[17] To first order in $\delta T\equiv T-T_0$ and $\delta P\equiv P-P_0$, where P_0 is the pressure corresponding to T_0, one finds $\tau_3(\text{sphere})=2\gamma_{sl}/L_0(r-t)=2\gamma_{sl}/L_0r_s$ and $\tau_3(\text{cylinder})=\gamma_{sl}/L_0(r-t)=\gamma_{sl}/L_0r_s$, when the Laplace-Young equation

$$P_s=P_l+\gamma_{sl}\left[\frac{1}{r_1}+\frac{1}{r_2}\right] \tag{6}$$

is used to express the pressure P_s of the solid phase in terms of the pressure P_l in the surrounding liquid phase, the solid-liquid surface tension γ_{sl}, and the principal radii of the surface curvature ($r_1=r_2\equiv r$ for a sphere, and $r_1=r$ while $r_2\rightarrow\infty$ for a cylinder).[1] If, as is often assumed, t is much smaller than r (and neglecting the difference between the surface free energy per unit area and the surface tension) then $\tau_3\approx\tau_2$. By comparing τ_3 with r_s^* one sees that the condition $\mu_s=\mu_l$ corresponds to $\delta F=\delta F^*$, and therefore is an unstable equilibrium.

In order to compare the measured size dependence of the pore In melting temperature with the preceding results, the measured melting temperature versus the inverse pore diameter has been plotted in Fig. 2(b). The solid straight line is a best fit to the data, and the predicted inverse pore size dependence of τ_1 and τ_2 is seen to describe the data reasonably well. The intercept of the best-fit straight line yields a value of $T(r\rightarrow\infty)=T_0=429.6$ K, in good agreement with the bulk In melting temperature of 429.8 K.[47] From the slope of Fig. 2(b) and τ_1, one obtains lower bounds of $f_{sl}=21$ mJ/m^2 for the spherical geometry of Fig. 4(a), and 32 mJ/m^2 for the cylindrical geometry of Fig. 4(b). Upper bounds of $f_{sl}=32$ mJ/m^2 and $f_{sl}=64$ mJ/m^2 for the spherical and cylindrical particle geometries are obtained from τ_2. Previous electron microscopy studies of the melting of small In particles in discontinuous films have resulted in values of $f_{sl}=110\pm20$ mJ/m^2 and 101 ± 10 mJ/m^2,[15,16] the former value being reported as an upper bound estimate. A value of $f_{sl}=30.8$ mJ/m^2 has also been reported based on undercooling experiments carried out on In droplets.[40]

If the melting of a small particle is an activated process, the peak in the heat-flow signal should shift in temperature in a nontrivial way (i.e., the shift should not simply be an experimental effect due to temperature lags in the calorimeter) as a function of the heating rate.[8] By analyzing the peak shift as a function of the heating rate, the activation energy can be estimated. The results of these measurements are shown in Fig. 6 for an In-CPG sample with $d=12.8$ nm. The displacement of the DSC melting signal corresponding to both the bulk and confined In is seen to be linear in the heating rate and is only due to thermal effects involving the flow of heat into or out of the DSC.[50] This result is not consistent with the presence of a significant energy barrier separating the liquid from the solid, and suggests that liquid In may be heterogeneously nucleated at the In-CPG wall.

An expression for a size-dependent latent heat can be derived starting from the definition $L=T(s_l-s_s)=(h_l-h_s)-(\mu_l-\mu_s)$, where $h(s,P)$ is the enthalpy per atom. Expanding $h(s,P)$ and $\mu(T,P)$ to first order in $\delta s\equiv s-s_0$, $\delta P\equiv P-P_0$, and $\delta T\equiv T-T_0$ yields a latent heat that depends on the ratio of the actual to fiducial melting temperature

$$L=\frac{T}{T_0}L_0=L_0\left[1-\frac{\alpha}{r}\right], \tag{7}$$

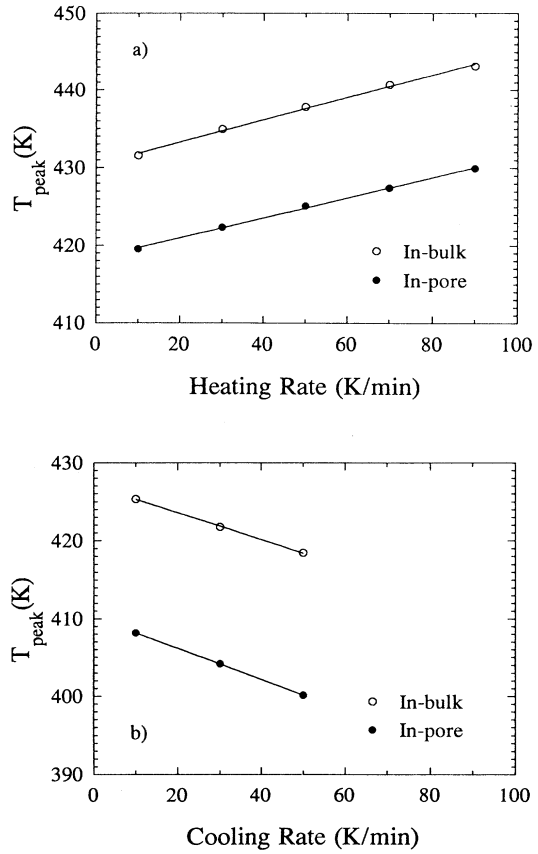

FIG. 6. Shift in the bulk (open circles) and pore (solid circles) In peak melting and freezing signals for a $d = 12.8$ nm In-CPG sample as a function of the heating and cooling rates.

where α is the coefficient of the r^{-1} term in the size-dependent melting temperature. In conjunction with the measured size dependence of the melting temperature, Eq. (7) predicts a latent heat in the 8.2-nm pore In sample of 26.3 J/gm, and in the 18.2-nm sample of 27.4 J/gm, rather than the measured values of 10.2 ± 0.4 and 14.7 ± 0.2 J/gm. Several possible explanations may account for the significant discrepancy between the predicted and measured values of the latent heat. In the first instance the mass of the pore In may have been overestimated, perhaps due to the formation of a nonmelting In-oxide layer next to the pore wall. This would require an oxide layer thickness between about 1.1 and 1.6 nm in the smaller pores, and between 1.6 and 2.4 nm in the larger pores for a cylindrical and spherical geometry, respectively. It should be noted, however, that the presence of a nonmelting In-oxide layer would also have the effect of decreasing the effective pore diameter and would have a large effect on the melting temperature versus inverse pore diameter plot of Fig. 2(b). In addition, no evidence for In-oxide, at least in a crystalline form, was found based on the x-ray-diffraction measurements of In-Vycor. Second, if the melting of the surface or near-surface regions of the pore In contributes a relatively smaller latent heat than does the interior region, the actual latent heat may be smaller than predicted by Eq. (7) where only a single bulk latent heat is assumed. These questions are currently under investigation in other small particle systems where the latent heat can more conveniently be measured over a wide range of pore sizes.

SUMMARY

The size-dependent melting and freezing behavior of pore In confined in porous silica glasses has been studied by differential scanning calorimetry over a wide range of pore sizes. The melting temperature of the pore In was found to be reduced in inverse proportion to the pore size, in good agreement with the results of a classical thermodynamic treatment of melting in finite systems. In the smallest pores, the latent heat was found to be reduced in comparison with the bulk value, but by an amount greater than expected based on a simple thermodynamic treatment which does not include a possible reduced latent heat for the surface region of the pore In. No evidence for activated melting behavior was found.

ACKNOWLEDGMENTS

We wish to thank Y. N. Wong and CPG, Inc. for providing the porous CPG glasses and the results of their Hg intrusion and nitrogen adsorption measurements. We also acknowledge J. R. Beamish, W. B. Daniels, E. Kerner, M. V. Moore, and J. F. Sheehan for useful conversations. The work of K.M.U. was supported in part by the Office of Naval Research under Contract No. N00014-88-K003. The work of T.E.H. and C.A.H. was supported by the Army Research Office through Grant No. DDA.LO3-91-G-0340. Additional support was provided by the National Science Foundation through Grant No. DMR 90-13127 (T.E.H.), and by the Naval Surface Warfare Center Independent Research Program (C.A.H.).

[1]See, e.g., R. Defay, I. Prigogine, A. Bellemans, and D. H. Everett, *Surface Tension and Adsorption* (Wiley, New York, 1966); D. P. Woodruff, *The Solid-Liquid Interface,* (Cambridge University Press, London, 1973); A. R. Ubbelohde, *The Molten State of Matter,* (Wiley, New York, 1978), and references therein.

[2]J. J. Thomson, *Applications of Dynamics to Physics and Chemistry,* (Dawsons of Pall Mall, London, 1968).

[3]P. Pawlow, Z. Phys. Chem. **65**, 545 (1909).

[4]H. Reiss and I. B. Wilson, J. Colloid Sci. **3**, 551 (1948).

[5]See, e.g., J. H. Hollomon and D. Turnbull, in *Progress in Metal Physics,* edited by B. Chalmers (Interscience, New York, 1953), Vol. 4, pp. 333–388.
[6]M. Takagi, J. Phys. Soc. Jpn. **9**, 359 (1954).
[7]See, e.g., J. H. Perepezko and I. E. Anderson, in *Synthesis and Properties of Metastable Phases,* edited by E. S. Machlin and T. J. Rowland (The Metallurgical Society, Warrendale, PA, 1980), pp. 31–63; J. H. Perepezko, B. A. Mueller, and K. Ohsaka, in *Undercooled Alloy Phases,* edited by E. W. Collings and C. C. Koch, Proceedings of the 1986 Hume-Rothery Memorial Symposium, New Orleans, 1986, edited by E. W. Collings and C. C. Koch (The Metallurgical Society, Warrendale, PA, 1987), pp. 289–320.
[8]K. F. Kelton, in *Solid State Physics,* edited by H. Ehrenreich and D. Turnbull (Academic, Boston, 1991), Vol. 45, pp. 75–177.
[9]W. Wildner, H.-D. Pfannes, and U. Gonser, J. Phys. (Paris) Colloq. **35**, C6-381 (1974).
[10]M. Blackman and A. E. Curzon, in *Structure and Properties of Thin Films,* edited by C. A. Neugebauer, J. B. Newkirk, and D. A. Vermilyea (Wiley, New York, 1959), pp. 217–222.
[11]C. R. M. Wronski, Brit. J. Appl. Phys. **18**, 1731 (1967).
[12]B. T. Boiko, A. T. Pugachev, and V. M. Bratsykhin, Fiz. Tverd. Tela (Leningrad) **10**, 3567 (1969) [Sov. Phys. Solid State **10**, 2832 (1969)].
[13]J. F. Pocza, A. Barna, and P. B. Barna, J. Vac. Sci. Technol. **6**, 472 (1969).
[14]J. R. Sambles, Proc. R. Soc. London, Ser. A **324**, 339 (1971); S. J. Peppiatt and J. R. Sambles, *ibid.* **345**, 387 (1975); S. J. Peppiatt, *ibid* **345**, 401 (1975).
[15]C. J. Coombes, J. Phys. F **2**, 441 (1972).
[16]R. P. Berman and A. E. Curzon, Can. J. Phys. **52**, 923 (1974).
[17]Ph. Buffat and J.-P. Borel, Phys. Rev. A **13**, 2287 (1976); Ph. Buffat, Thin Solid Films **32**, 283 (1976).
[18]G. L. Allen, W. W. Gile, and W. A. Jesser, Acta Metall. **28**, 1695 (1980).
[19]G. L. Allen, R. A. Bayles, W. W. Gile, and W. A. Jesser, Thin Solid Films **144**, 297 (1986).
[20]Y. Lereah, G. Deutscher, and R. Kofman, Europhys. Lett. **8**, 53 (1989).
[21]P. Cheyssac, R. Kofman, and R. Garrigos, Solid State Commun. **44**, 1583 (1982); R. Garrigos, R. Kofman, P. Cheyssac, and M. Y. Perrin, Europhys. Lett. **1**, 355 (1986).
[22]K. M. Unruh, B. M. Patterson, and S. I. Shah, J. Mater. Res. **7**, 214 (1992), B. M. Patterson, K. M. Unruh, and S. I. Shah, Nanostruct. Mater. **1**, 65 (1992).
[23]C. C. Koch, J. S. C. Jang, and S. S. Gross, J. Mater. Res. **4**, 557 (1989); J. S. C. Jang and C. C. Koch, *ibid* **5**, 325 (1990).
[24]L. Grabaek, J. Bohr, E. Johnson, A. Johansen, L. Sarholt-Kristensen, and H. H. Andersen, Phys. Rev. Lett. **64**, 934 (1990).
[25]T. Castro, R. Reifenberger, E. Choi, and R. P. Andres, Phys. Rev. B **42**, 8548 (1990).
[26]See, e.g., W. Haller, in *Solid Phase Biochemistry: Analytic and Synthetic Aspects,* edited by W. H. Scouten (Wiley, New York, 1983), Chap. 11.
[27]CPG Inc., 32 Pier Lane West, Fairfield, NJ 07006.
[28]J. L. Tell and H. J. Maris, Phys. Rev. B **28**, 5122 (1983).
[29]R. H. Torii, H. J. Maris, and G. M. Seidel, Phys. Rev. B **41**, 7167 (1990).
[30]D. F. Brewer, J. Rajendra, N. Sharma, and A. L. Thomson, Physica B **165&166**, 569 (1990).
[31]For references to early He studies, see D. F. Brewer, in *Superfluid Helium,* edited by J. F. Allen (Academic, New York, 1966), pp. 159–177; D. F. Brewer, J. Low Temp. Phys. **3**, 205 (1970); D. F. Brewer, A. Evenson, and A. L. Thomson, *ibid.* **3**, 603 (1970); D. F. Brewer, J. Rajendra, N. Sharma, A. L. Thomson, and J. Xin, Physica B **165&166**, 551 (1990); D. F. Brewer, J. Rajendra, N. Sharma, A. L. Thomson, and J. Xin, *ibid.* **165&166**, 577 (1990).
[32]R. H. Tait and J. D. Reppy, Phys. Rev. B **20**, 997 (1979).
[33]E. D. Adams, K. Uhlig, Y.-H. Tang, and G. E. Haas, Phys. Rev. Lett. **52**, 2249 (1984); E. D. Adams, Y.-H. Tang, K. Uhlig, and G. E. Haas, J. Low Temp. Phys. **66**, 85 (1987).
[34]G. Litvan and R. McIntosh, Can. J. Chem. **41**, 3095 (1963).
[35]W. A. Patrick and W. A. Kemper, J. Phys. Chem. **42**, 369 (1938).
[36]C. Hodgson and R. McIntosh, Can. J. Chem. **38**, 958 (1960).
[37]A. A. Antoniou, J. Phys. Chem. **68**, 2754 (1964); G. G. Litvan, Can. J. Chem. **44**, 2617 (1966); G. K. Rennie and J. Clifford, J. Chem. Soc. F1 **73**, 680 (1977).
[38]C. L. Jackson and G. B. McKenna, J. Chem. Phys. **93**, 9002 (1990).
[39]R. Mu and V. M. Malhotra, Phys. Rev. B **44**, 4296 (1991).
[40]V. P. Skripov, in *Crystal Growth and Materials,* edited by E. Kaldis and H. J. Scheel (North-Holland, Amsterdam, 1977), pp. 328–378.
[41]Corning Glass Works, Corning, NY 14830.
[42]Micromeritics Instrument Corporation, One Micromeritics Drive, Norcross, GA 30093-1877.
[43]See, e.g., M. L. Hair, *Infrared Spectroscopy in Surface Chemistry* (Marcel Dekker, New York, 1967).
[44]C. A. Huber and T. E. Huber, J. Appl. Phys. **64**, 6588 (1988).
[45]T. E. Huber, P. W. Schmidt, J.-S. Lin, and C. A. Huber, in *Scaling in Disordered Materials: Fractal Structure and Dynamics,* edited by J. P. Stokes, M. O. Robbins, and T. A. Witten, Symposia Proceedings No. EA-25 (Materials Research Society, Pittsburgh, 1990), pp. 207–210.
[46]Perkin-Elmer Corporation, 761 Main Avenue, Norwalk, CT 06856-9966.
[47]See, e.g., *CRC Handbook of Chemistry and Physics, 72nd ed.* (CRC, Boca Raton, FL, 1991).
[48]P. R. Couchman and W. A. Jesser, Nature **269**, 481 (1977).
[49]V. P. Koverda, V. N. Skokov, and V. P. Skripov, Fiz. Met. Metalloved. **51**, 1238 (19xx) [Phys. Met. Metallogr. **51**, 97 (1981)]; V. P. Skripov, V. P. Koverda, and V. N. Skokov, Phys. Status Solidi A **66**, 109 (1981).
[50]Perkin-Elmer Corporation, Thermal Analysis Newsletter, No. 9 (1970).